JACS
JOURNAL OF THE AMERICAN CHEMICAL SOCIETY
pubs.acs.org/JACS
Article

Selective Formation of Acetic Acid and Methanol by Direct Methane Oxidation Using Rhodium Single-Atom Catalysts

Haoyi Li, Chuanye Xiong, Muchun Fei, Lu Ma, Hongna Zhang, Xingxu Yan, Peter Tieu, Yucheng Yuan, Yuhan Zhang, James Nyakuchena, Jier Huang, Xiaoqing Pan, Matthias M. Waegele, De-en Jiang,* and Dunwei Wang*

Cite This: *J. Am. Chem. Soc.* 2023, 145, 11415−11419
Read Online

ABSTRACT: Atomically dispersed catalysts such as single-atom catalysts have been shown to be effective in selectively oxidizing methane, promising a direct synthetic route to value-added oxygenates such as acetic acid or methanol. However, an important challenge of this approach has been that the loading of active sites by single-atom catalysts is low, leading to a low overall yield of the products. Here, we report an approach that can address this issue. It utilizes a metal−organic framework built with porphyrin as the linker, which provides high concentrations of binding sites to support atomically dispersed rhodium. It is shown that up to 5 wt% rhodium loading can be achieved with excellent dispersity. When used for acetic acid synthesis by methane oxidation, a new benchmark performance of 23.62 mmol·g_{cat}^{-1}·h^{-1} was measured. Furthermore, the catalyst exhibits a unique sensitivity to light, producing acetic acid (under illumination, up to 66.4% selectivity) or methanol (in the dark, up to 65.0% selectivity) under otherwise identical reaction conditions.

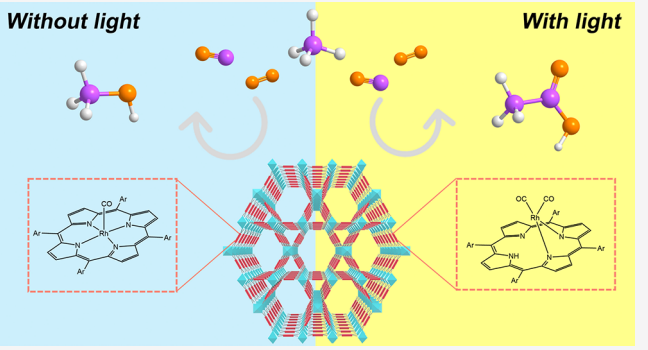

INTRODUCTION

As an abundant natural resource, methane (CH_4) is an appealing feedstock for the synthesis of value-added oxygenates such as methanol (CH_3OH) and acetic acid (CH_3COOH).[1−3] However, due to the difficulties in selectively activating the first C−H bond without overoxidizing CH_4, it has been exceedingly challenging to achieve the synthesis of these oxygenates through direct CH_4 oxidation.[4,5] Existing industrial processes instead rely on reforming CH_4 to first produce syngas, a route that is indirect, energy intense, and highly polluting.[2,6] The issues are exemplified by state-of-the-art production of CH_3COOH, which requires CH_3OH as a precursor, the synthesis of which involves first oxidizing CH_4 to syngas.[7,8] In principle, the synthesis of CH_3COOH can be greatly simplified by directly activating CH_4, followed by oxidative carbonylation. Indeed, this route has attracted significant research attention lately. It has been found that when atomically dispersed catalysts such as rhodium single-atom catalysts (Rh SACs) are used, selective activation of CH_4 can be achieved for the direct production of CH_3COOH.[9,10] Nevertheless, the performance as measured by yield per catalyst weight remains low, limiting its prospect for practical applications. An important reason for the relatively low yield by Rh SACs lies in the nature of the catalyst itself. It is reported that selective CH_4 activation is only favored when the Rh active center is atomically dispersed; the presence of Rh clusters would favor CH_4 overoxidation.[11,12] To date, the highest performing Rh SACs were obtained on a zeolite support (ZSM-5), onto which a low loading (up to 0.5 wt %) of dispersed Rh SACs is possible.[9] It has been argued that the low loading is due to the relatively weak binding between Rh atoms and zeolites; further increasing the Rh loading would result in aggregated Rh clusters and, hence, a lower yield of CH_3COOH formation.[13,14] In fact, how to maximize SAC loading represents a broader challenge that has been actively studied recently. The most successful demonstrations to date have been achieved on carbon-based support for electrocatalytic applications,[15,16] in which the binding sites often involve N heteroatoms. Inspired by advances in these parallel fields, here, we report a method to prepare high-loading Rh SACs for the synthesis of CH_3COOH by direct CH_4 transformation. Our strategy takes advantage of the high concentration of porphyrin functional groups in a metal−organic framework (MOF) support. These porphyrin sites are effective in dispersing Rh atoms, allowing for up to 5 wt %

Received: March 25, 2023
Published: May 12, 2023

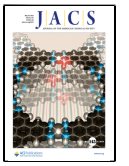

https://doi.org/10.1021/jacs.3c03113
J. Am. Chem. Soc. 2023, 145, 11415−11419

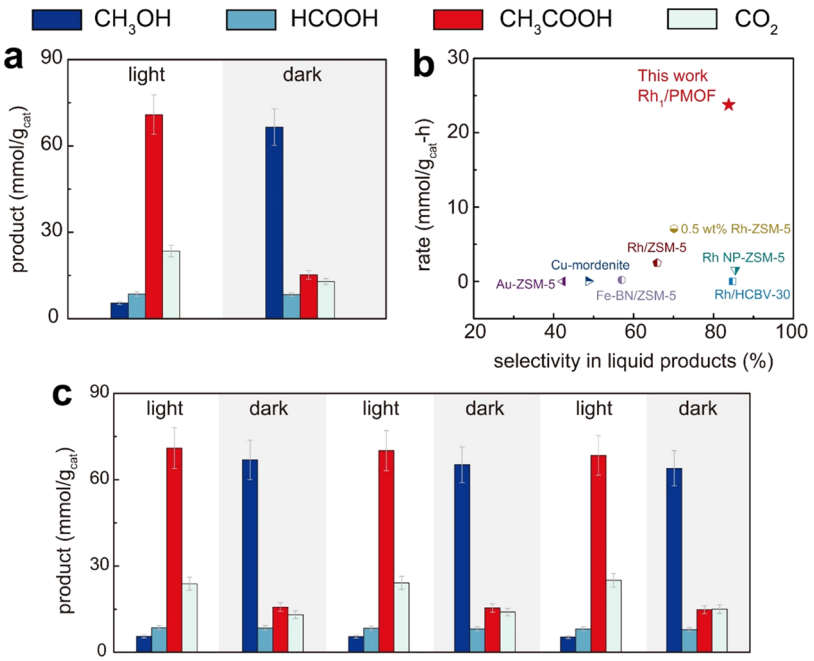

Figure 1. (a) Catalytic performance in light (left) and dark (right) showing the dominant products of CH_3COOH and CH_3OH, respectively, in a 3 h reaction. (b) Literature comparison of the formation rate of CH_3COOH by CH_4 oxidation on heterogeneous catalysts. References are as follows: Au-ZSM-5;[17] Cu-mordenite;[18] Fe-BN/ZSM-5;[19] Rh/ZSM-5;[10] 0.5 wt % Rh-ZSM-5;[9] Rh NP-ZSM-5;[20] and Rh/HCBV-30.[21] (c) Reversible selectivity switch between CH_3COOH and CH_3OH in light and dark, respectively, with the same batch of catalyst. Each run was conducted for 3 h. Reaction conditions: 20 mg of Rh_1/pMOF, 4 bar O_2, 5 bar CO, 15 bar CH_4, 20 mL of water, 150 °C as the reaction temperature. Light: 100 mW/cm^2, AM 1.5G. Error bars represent the standard deviations of at least three repeated experiments under the same conditions.

loading of Rh SACs. The resulting catalysts exhibited outstanding performance in converting CH_4 to CH_3COOH, increasing the previous benchmark record by more than 2-fold to 71.27 mmol·g_{cat}^{-1} for a typical 3 h reaction. Moreover, the catalyst showed a unique sensitivity to light. Under otherwise identical reaction conditions, it favored CH_3COOH formation (up to 66.4% selectivity) under illumination but CH_3OH formation (up to 65.0% selectivity) in the dark. Importantly, the selectivity switch is highly reversible by tuning the light on and off.

RESULTS AND DISCUSSION

The preparation of porphyrin-based MOF (denoted as pMOF hereafter) followed a previous report,[22] and the resulting product was a rod-shaped crystal (Figures S1 and S2). Afterward, Rh was loaded into tetrakis(4-carboxyphenyl) porphyrin (TCPP) binding pockets through a wet impregnation method with rhodium chloride ($RhCl_3$) as the precursor (Figures S2 and S3). It was found that up to 5.04 wt % Rh loading could be achieved by repeating the impregnation process 5 times. This loading is close to the theoretical limit of 7.73 wt % (see the Supporting Information for more discussions). This result represents a more significant increase of Rh loading than Rh SACs on ZSM-5.[9,10]

Our next task was to confirm that Rh was atomically dispersed in pMOF. For this purpose, we first carried out extended X-ray absorption fine structure (EXAFS) characterization. As shown in Figures S4, S5 and Table S1, no Rh−Rh bonding was detected, while the coordination between Rh and N, as well as that between Rh and Cl, was apparent. This finding serves as direct evidence that no measurable Rh clusters were formed, and Rh atoms were anchored at the porphyrin binding pockets. Further supporting this understanding was the carbon monoxide-based diffuse reflectance infrared Fourier transform spectroscopy (CO-DRIFTS). No absorption peaks of CO were measured in the region between 1800 and 1950 cm^{-1} (Figure S6), which suggests the absence of Rh clusters.[23] The sample was also examined by aberration-corrected high-angle annular dark field scanning transmission electron microscopy (AC HAADF-STEM), and no apparent Rh clusters were observed (Figure S3). Together, these data provide strong evidence that atomically dispersed Rh atoms were obtained on pMOF. The information helped us propose the coordination environment of Rh (*vide infra*).

With the structure and stability of the Rh_1/pMOF established, we next studied the competency of the system to catalyze CH_3COOH synthesis. For this purpose, we also tested the thermostability of the catalyst by thermogravimetric analysis (TGA). No apparent phase transition or decomposition was observed below 400 °C (Figure S7). In a typical experiment of CH_3COOH synthesis, 20 mg of Rh_1/pMOF was dispersed in 20 mL of deionized H_2O in a pressurized reactor (capacity: 3 oz; see the Supporting Information for more details). The reactor was then pressurized with 15 bar CH_4, 5 bar CO, and 4 bar O_2. It was heated to 150 °C in a silicone oil bath and kept at this temperature for 3 h. With illumination by a solar simulator (Solar Light, model 16S-300-3-AM, at 100 mW/cm^2 intensity), 1.42 mmol of CH_3COOH was measured; other detectable products included 0.11 mmol of CH_3OH, 0.17 mmol of formic acid (HCOOH), and 0.47 mmol of carbon dioxide (CO_2) (Figures 1a and S8 and S9). The calculated conversion of CH_4 in a typical 3 h reaction was ca. 5.22% (Table S2). The normalized rate of 23.62 mmol·g_{cat}^{-1}·h^{-1} for CH_3COOH production represents a significant increase of the previous benchmark under similar conditions but without light illumination (Figure 1b). The total selectivity

https://doi.org/10.1021/jacs.3c03113
J. Am. Chem. Soc. 2023, 145, 11415−11419

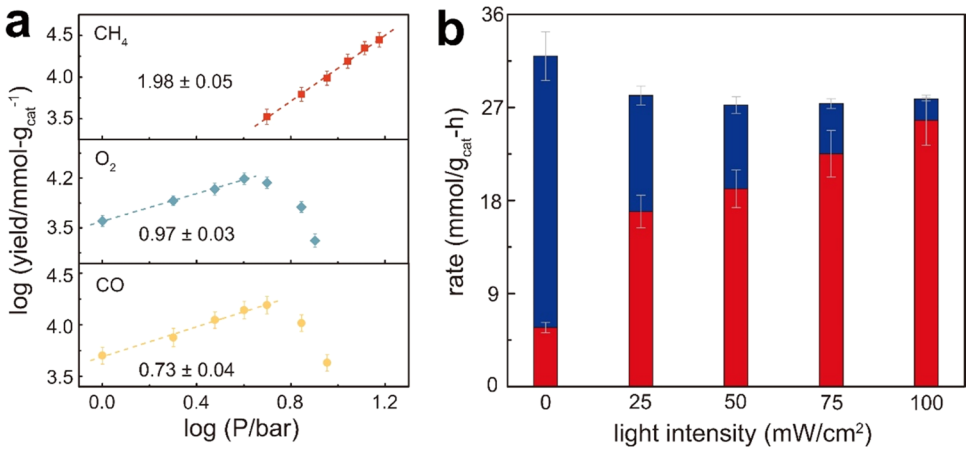

Figure 2. (a) Relationship between partial pressures of reactants and the yield of CH_3COOH for a fixed duration of 45 min plotted in logarithmic scales. Reaction conditions: 20 mg of Rh_1/pMOF, varying partial pressures of O_2, CO, and CH_4, where the total pressure was maintained at 24 bar by using Ar as a balancing gas, 20 mL of water, 150 °C as the reaction temperature. Light: 100 mW/cm^2, AM 1.5G. (b) Relationship between the formation rate of CH_3COOH (red) and CH_3OH (blue) with varying light intensities. Reaction conditions: 20 mg of Rh_1/pMOF, 4 bar O_2, 5 bar CO, 15 bar CH_4, 20 mL of water, 150 °C as the reaction temperature, 1 h as the reaction time. Error bars represent the standard deviations of at least three repeated experiments under the same conditions.

toward liquid products (83.81%) is also among the highest in the literature. When normalized to per Rh atom, a higher activity (74.97 mol·mol$_{Rh}^{-1}$·h^{-1}) was obtained on Rh_1/pMOF with a lower loading (0.5 wt %), which is comparable to that reported in ref 9. The value for high-loading Rh_1/pMOF was 48.24 mol·mol$_{Rh}^{-1}$·h^{-1}, which is lower than that by low-loading Rh catalysts presumably due to mass transport limitations of the reactants or the products or both. Future research will be needed to further optimize the loading to maximize both the overall and normalized activities. Lastly, to understand the mechanisms and identify the source of carbon in the products, we performed $^{13}CH_4$ and ^{13}CO isotope-labeled synthesis (Figure S10). These results suggest that CH_4 mainly contributes to the formation of methyl in the product CH_3COOH, whereas CO forms the carbonyl function group.

As an initial effort to optimize the reaction conditions for the synthesis of CH_3COOH, the partial pressures of the three key reactants were independently varied (Figures S11−S17). As shown in Figure 2a, when the CH_4 pressure (P_{CH_4}) was changed between 5 and 15 bar, the reaction rate exhibited a second-order dependence on P_{CH_4} (Figure S11). Similarly, when the O_2 pressure (P_{O_2}) was changed between 1 and 4 bar, the reaction rate showed a first-order dependence on P_{O_2}. Further increasing P_{O_2} beyond 4 bar, however, led to overoxidation of CH_4 and to an obvious decrease of the CH_3COOH yield (Figure S12). While a similar trend of the reaction rate with CO pressure (P_{CO}) was observed between P_{CO} = 1 and 5 bar, the dependence was significantly lower (with an apparent order of 0.73) than the expected second-order relationship as predicted by the stoichiometry, suggesting that the catalyst may already be saturated with CO. Further increasing P_{CO} beyond 5 bar resulted in a dramatic increase of CO_2 production at the expense of selectivity toward CH_3COOH, presumably due to the blocking of active sites by the oversaturation of CO (Figure S13). The reaction temperature was also varied (Figure S18). The general trend was that the higher the temperature, the higher the rate of CH_3COOH production. An apparent activation barrier of 22.3 kJ/mol was calculated based on this set of data (Figure S19). The lowest temperature at which CH_3COOH was detectable was 70 °C. Further increasing the temperature beyond 150 °C led to an increase of CO_2 production and an apparent decrease of selectivity toward CH_3COOH (Figure S20).

To study the effects of light on the reaction, a similar process was carried out under identical conditions but without light. Substantially different selectivity of products was measured, 65% of which was CH_3OH, and only 14.8% of the product was CH_3COOH (Figure 1a). The striking change of selectivity with and without illumination is highly unique. A similar phenomenon has not been reported in the literature, to the best of our knowledge. Critically, such a switch is highly reversible. As evidence, we show in Figure 1c that the change of selectivity (*ca.* 64.7% average selectivity to CH_3COOH in light and ca. 63.5% average selectivity to CH_3OH in dark) was reproducible on the same batch of catalysts for at least 6 cycles. This group of experiments also revealed the stability of the catalyst for extended reaction times. Indeed, control experiments showed that similar performance of CH_3COOH production (with light) was measured on Rh_1/pMOF for at least 7 cycles with 3 h reaction for each cycle (Figure S21). Likewise, comparable production of CH_3OH (without light) was obtained for at least 7 cycles (Figure S22). It is worth noting that similar rates and selectivity were measured for single-step reactions with duration up to 20 h (Figures S23 and S24). Also supporting the stability of the catalyst were the CO-DRIFTS spectra, which revealed minimum aggregation of Rh atoms after catalysis (Figure S6). This conclusion is consistent with other spectroscopic and electroscopic characterizations of the catalysts, as well (Figures S2, S4, and S25−S28).

While the high performance of Rh_1/pMOF in the CH_3COOH synthesis by direct CH_4 oxidation may be expected owing to the high density of atomically dispersed Rh sites, the switch of product selectivity between CH_3COOH and CH_3OH with and without light, respectively, is new and intriguing. To gain insights into the possible origin of this switch, we next turned to density functional theory (DFT) calculations. In doing so, we examined two reported coordination environments of Rh in a porphyrin binding site (Figure S29),[24] namely, the in-plane geometry (Figure S30)

https://doi.org/10.1021/jacs.3c03113
J. Am. Chem. Soc. 2023, 145, 11415−11419

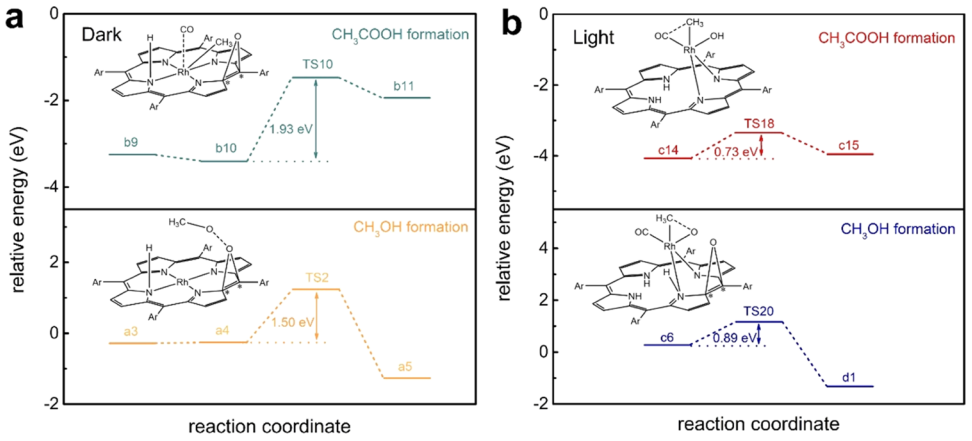

Figure 3. (a) Preinsertion step of CO for the formation of CH_3COOH (upper) and the O_2 dissociation step for the formation of CH_3OH (bottom) at the in-plane Rh_1 site. (b) Methyl migration to CO for the formation of CH_3COOH (upper) and methyl migration to O for the formation of CH_3OH (bottom) at the out-of-plane Rh_1 site. The steps in a and b are referred to those in the overall catalytic cycles as shown in Figures S31 and S33, respectively. Inset structures in a and b show the corresponding transition states.

and the out-of-plane one (Figure S6). Our calculations suggest that the in-plane Rh_1 site favors CH_3OH formation, whereas CH_3COOH production is favored by the out-of-plane Rh_1 site. As shown in Figures S31 and S32, the difficulty of CH_3COOH formation at the in-plane Rh_1 site lies in the high activation energy of CO coadsorption next to CH_3 on Rh_1 in preparation for the insertion step (TS10 in Figure 3a). For the out-of-plane Rh_1 site, the key differentiating step between CH_3OH formation and that of CH_3COOH is methyl migration, as shown in Figure 3b (see also Figures S33 and S34), where CH_3COOH production is favored. It is further noted that the DFT calculations were conducted with simplifications, and the activation barriers reported here should be treated qualitatively for the purpose of comparing different product selectivities (see the Supporting Information for more discussions). While additional research will be required to fully understand the process, we hypothesize that light-induced ligand-to-metal charge transfer (LMCT) is the key factor that leads to the changes of the Rh coordination environment under reaction conditions.[25−27] LMCT was indeed observed by transient ultraviolet−visible (UV−vis) absorption spectroscopy (Figure S35). Moreover, the selectivity is dependent on light intensity in a monotonic fashion, as shown in Figure 2b, suggesting that the portion of active sites that adopts the out-of-plane coordination environment is proportional to light intensities.

CONCLUSIONS

In summary, we have developed a strategy to maximize Rh SAC loading for a new benchmark in acetic acid synthesis by selective methane oxidation. This approach takes advantage of the binding sites of porphyrin in a MOF support. Uniquely, the catalysts showed stark selectivity differences with or without light, producing predominantly acetic acid or methanol, respectively. The results opened a new door toward methane valorization.

ASSOCIATED CONTENT

Supporting Information

The Supporting Information is available free of charge at https://pubs.acs.org/doi/10.1021/jacs.3c03113.

Experimental methods and characterizations; X-ray diffraction (XRD) patterns; CO-DRIFTS spectra; TGA−differential scanning calorimetry (TGA−DSC) spectrum; isotope labeling experimental results; EXAFS fitting results; AC HAADF-STEM images; EDS elemental maps; X-ray absorption near edge spectroscopy (XANES) spectra; additional catalytic data; and DFT calculations (PDF)

AUTHOR INFORMATION

Corresponding Authors

De-en Jiang − *Department of Chemistry, University of California, Riverside, California 92521, United States*; Email: djiang@ucr.edu

Dunwei Wang − *Department of Chemistry, Boston College, Chestnut Hill, Massachusetts 02467, United States*; orcid.org/0000-0001-5581-8799; Email: dunwei.wang@bc.edu

Authors

Haoyi Li − *Department of Chemistry, Boston College, Chestnut Hill, Massachusetts 02467, United States*; orcid.org/0000-0002-0723-8068

Chuanye Xiong − *Department of Chemistry, University of California, Riverside, California 92521, United States*

Muchun Fei − *Department of Chemistry, Boston College, Chestnut Hill, Massachusetts 02467, United States*

Lu Ma − *National Synchrotron Light Source II, Brookhaven National Laboratory, Upton, New York 11973, United States*

Hongna Zhang − *Department of Chemistry, Boston College, Chestnut Hill, Massachusetts 02467, United States*

Xingxu Yan − *Department of Materials Science and Engineering, University of California, Irvine, California 92697, United States; Irvine Materials Research Institute, University of California, Irvine, California 92697, United States*; orcid.org/0000-0001-7991-4849

Peter Tieu − *Department of Chemistry, University of California, Irvine, California 92697, United States*; orcid.org/0000-0001-8727-2313

Yucheng Yuan − *Department of Chemistry, Boston College, Chestnut Hill, Massachusetts 02467, United States*; orcid.org/0000-0003-3935-0967

Yuhan Zhang − *Department of Chemistry, Boston College, Chestnut Hill, Massachusetts 02467, United States*

James Nyakuchena − *Department of Chemistry, Marquette University, Milwaukee, Wisconsin 53201, United States*
Jier Huang − *Department of Chemistry, Marquette University, Milwaukee, Wisconsin 53201, United States;* orcid.org/0000-0002-2885-5786
Xiaoqing Pan − *Department of Materials Science and Engineering, University of California, Irvine, California 92697, United States; Irvine Materials Research Institute and Department of Physics and Astronomy, University of California, Irvine, California 92697, United States;* orcid.org/0000-0002-0965-8568
Matthias M. Waegele − *Department of Chemistry, Boston College, Chestnut Hill, Massachusetts 02467, United States;* orcid.org/0000-0002-1186-7545

Complete contact information is available at: https://pubs.acs.org/10.1021/jacs.3c03113

Notes

The authors declare no competing financial interest.

■ ACKNOWLEDGMENTS

The work was funded by the National Science Foundation (CBET-1924689 to Boston College and CBET-1924545 to UC Riverside). The authors thank Prof. J. A. Byers at Boston College for his support of the TGA measurements. X-ray absorption spectroscopy studies used resources of the National Synchrotron Light Source II, a U.S. Department of Energy (DOE) Office of Science User Facility operated for the DOE Office of Science by Brookhaven National Laboratory under Contract No. DE-SC0012704. The authors acknowledge the use of facilities and instrumentation at the UC Irvine Materials Research Institute (IMRI), which is supported in part by the National Science Foundation through the UC Irvine Materials Research Science and Engineering Center (DMR-2011967).

■ REFERENCES

(1) Song, H.; Meng, X.; Wang, Z.-J.; Liu, H.; Ye, J. Solar-energy-mediated methane conversion. *Joule* **2019**, *3*, 1606−1636.
(2) Meng, X.; Cui, X.; Rajan, N. P.; Yu, L.; Deng, D.; Bao, X. Direct methane conversion under mild condition by thermo-, electro-, or photocatalysis. *Chem* **2019**, *5*, 2296−2325.
(3) Le Berre, C.; Serp, P.; Kalck, P.; Torrence, G. P. Acetic Acid. In *Ullmann's Encyclopedia of Industrial Chemistry*; John Wiley & Sons, Inc., 2014; pp 1−34.
(4) Yuliati, L.; Yoshida, H. Photocatalytic conversion of methane. *Chem. Soc. Rev.* **2008**, *37*, 1592−1602.
(5) Freakley, S. J.; Dimitratos, N.; Willock, D. J.; Taylor, S. H.; Kiely, C. J.; Hutchings, G. J. Methane oxidation to methanol in water. *Acc. Chem. Res.* **2021**, *54*, 2614−2623.
(6) Behrens, M.; Studt, F.; Kasatkin, I.; Kühl, S.; Hävecker, M.; Abild-Pedersen, F.; Zander, S.; Girgsdies, F.; Kurr, P.; Kniep, B.-L.; Tovar, M.; Fischer, R. W.; Nørskov, J. K.; Schlögl, R. The active site of methanol synthesis over $Cu/ZnO/Al_2O_3$ industrial catalysts. *Science* **2012**, *336*, 893−897.
(7) Kalck, P.; Le Berre, C.; Serp, P. Recent advances in the methanol carbonylation reaction into acetic acid. *Coord. Chem. Rev.* **2020**, *402*, No. 213078.
(8) Ravi, M.; Ranocchiari, M.; van Bokhoven, J. A. The direct catalytic oxidation of methane to methanol—A critical assessment. *Angew. Chem., Int. Ed.* **2017**, *56*, 16464−16483.
(9) Shan, J.; Li, M.; Allard, L. F.; Lee, S.; Flytzani-Stephanopoulos, M. Mild oxidation of methane to methanol or acetic acid on supported isolated rhodium catalysts. *Nature* **2017**, *551*, 605−608.
(10) Tang, Y.; Li, Y.; Fung, V.; Jiang, D.-E.; Huang, W.; Zhang, S.; Iwasawa, Y.; Sakata, T.; Nguyen, L.; Zhang, X.; Frenkel, A. I.; Tao, F. F. Single rhodium atoms anchored in micropores for efficient transformation of methane under mild conditions. *Nat. Commun.* **2018**, *9*, No. 1231.
(11) Bai, S.; Liu, F.; Huang, B.; Li, F.; Lin, H.; Wu, T.; Sun, M.; Wu, J.; Shao, Q.; Xu, Y.; Huang, X. High-efficiency direct methane conversion to oxygenates on a cerium dioxide nanowires supported rhodium single-atom catalyst. *Nat. Commun.* **2020**, *11*, No. 954.
(12) Kwon, Y.; Kim, T. Y.; Kwon, G.; Yi, J.; Lee, H. Selective activation of methane on single-atom catalyst of rhodium dispersed on zirconia for direct conversion. *J. Am. Chem. Soc.* **2017**, *139*, 17694−17699.
(13) Sui, X.; Zhang, L.; Li, J.; Doyle-Davis, K.; Li, R.; Wang, Z.; Sun, X. Advanced Support Materials and Interactions for Atomically Dispersed Noble-Metal Catalysts: From Support Effects to Design Strategies. *Adv. Energy Mater.* **2022**, *12*, No. 2102556.
(14) Wang, K.; Wang, X.; Liang, X. Synthesis of high metal loading single atom catalysts and exploration of the active center structure. *ChemCatChem* **2021**, *13*, 28−58.
(15) Hai, X.; Xi, S.; Mitchell, S.; Harrath, K.; Xu, H.; Akl, D. F.; Kong, D.; Li, J.; Li, Z.; Sun, T.; et al. Scalable two-step annealing method for preparing ultra-high-density single-atom catalyst libraries. *Nat. Nanotechnol.* **2022**, *17*, 174−181.
(16) Xia, C.; Qiu, Y.; Xia, Y.; Zhu, P.; King, G.; Zhang, X.; Wu, Z.; Kim, J. Y. T.; Cullen, D. A.; Zheng, D.; et al. General synthesis of single-atom catalysts with high metal loading using graphene quantum dots. *Nat. Chem.* **2021**, *13*, 887−894.
(17) Qi, G.; Davies, T. E.; Nasrallah, A.; Sainna, M. A.; Howe, A. G.; Lewis, R. J.; Quesne, M.; Catlow, C. R. A.; Willock, D. J.; He, Q.; Bethell, D.; Howard, M. J.; Murrer, B. A.; Harrison, B.; Kiely, C. J.; Zhao, X.; Deng, F.; Xu, J.; Hutchings, G. J. Au-ZSM-5 catalyses the selective oxidation of CH_4 to CH_3OH and CH_3COOH using O_2. *Nat. Catal.* **2022**, *5*, 45−54.
(18) Narsimhan, K.; Michaelis, V. K.; Mathies, G.; Gunther, W. R.; Griffin, R. G.; Roman-Leshkov, Y. Methane to acetic acid over Cu-exchanged zeolites: mechanistic insights from a site-specific carbonylation reaction. *J. Am. Chem. Soc.* **2015**, *137*, 1825−1832.
(19) Wu, B.; Lin, T.; Lu, Z.; Yu, X.; Huang, M.; Yang, R.; Wang, C.; Tian, C.; Li, J.; Sun, Y.; Zhong, L. Fe binuclear sites convert methane to acetic acid with ultrahigh selectivity. *Chem* **2022**, *8*, 1658−1672.
(20) Moteki, T.; Tominaga, N.; Ogura, M. CO-Assisted Direct Methane Conversion into C_1 and C_2 Oxygenates over ZSM-5 Supported Transition and Platinum Group Metal Catalysts Using Oxygen as an Oxidant. *ChemCatChem* **2020**, *12*, 2957−2961.
(21) Golubev, K. B.; Yashina, O.; Batova, T.; Kolesnichenko, N.; Ezhova, N. Direct Low-Temperature Oxidative Conversion of Methane to Acetic Acid on Rhodium-Modified Zeolites. *Pet. Chem.* **2021**, *61*, 663−669.
(22) He, T.; Chen, S.; Ni, B.; Gong, Y.; Wu, Z.; Song, L.; Gu, L.; Hu, W.; Wang, X. Zirconium−porphyrin-based metal−organic framework hollow nanotubes for immobilization of noble-metal single atoms. *Angew. Chem., Int. Ed.* **2018**, *130*, 3551−3556.
(23) Matsubu, J. C.; Yang, V. N.; Christopher, P. Isolated metal active site concentration and stability control catalytic CO_2 reduction selectivity. *J. Am. Chem. Soc.* **2015**, *137*, 3076−3084.
(24) Thompson, S. J.; Brennan, M. R.; Lee, S. Y.; Dong, G. Synthesis and applications of rhodium porphyrin complexes. *Chem. Soc. Rev.* **2018**, *47*, 929−981.
(25) Leng, F.; Liu, H.; Ding, M.; Lin, Q.-P.; Jiang, H.-L. Boosting photocatalytic hydrogen production of porphyrinic MOFs: the metal location in metalloporphyrin matters. *ACS Catal.* **2018**, *8*, 4583−4590.
(26) Kim, D.; Whang, D. R.; Park, S. Y. Self-Healing of Molecular Catalyst and Photosensitizer on Metal−Organic Framework: Robust Molecular System for Photocatalytic H_2 Evolution from Water. *J. Am. Chem. Soc.* **2016**, *138*, 8698−8701.
(27) Horváth, O.; Valicsek, Z.; Harrach, G.; Lendvay, G.; Fodor, M. A. Spectroscopic and photochemical properties of water-soluble metalloporphyrins of distorted structure. *Coord. Chem. Rev.* **2012**, *256*, 1531−1545.